

Study on the Spatial Damage Characteristics of Working Fluid in a Sandstone Reservoir and an Unplugged Fluid System

Xiaozhi Xin, Jinming Zhao, Yiwen Xu, Chenghong Jin, Zhifeng Luo, Yiming Wang, and Haoran Fu*

Cite This: *ACS Omega* 2024, 9, 18400–18411

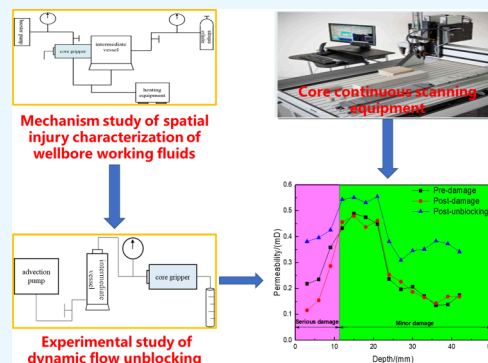
Read Online

ACCESS |

Metrics & More

Article Recommendations

ABSTRACT: Due to its good physical properties and low pressure coefficient, the K75 reservoir is prone to leakage and intrusion of drilling and completion fluids during well construction, resulting in plugging of the borehole throat, which will inevitably affect the injection and recovery capacity of the gas well. In order to ensure the strong injection and production capacity of the K75 reservoir, this paper clarifies the reservoir space damage characteristics under different pressure differences and different entry fluids by establishing physical simulation of the damage, selecting the optimal system of the decongestant, and conducting dynamic flow decongestion experiments, as well as combining with the characterization means of the continuous scanning system of the core and the permeability test of the gas measurement. The test results show that the degree of damage of the same working fluid increases with the increase of differential pressure of repulsion, and the degree of damage of sequential working fluids (drilling fluid, completion fluid, and perforating fluid) is greater than that of drilling fluid damage under the same differential pressure of repulsion. In order to relieve the damage of wellbore working fluids, a set of multifunctional, low-corrosion composite acid system formulas was selected through rock powder, mud cake dissolution experiments, and dynamic flow unblocking experiments; the permeability recovery rate of this acid system after unblocking was more than 90%, which is widely applicable, and it is useful for the acidizing and unblocking practice in similar reservoirs.



1. INTRODUCTION

In the drilling process of oil and gas wells, working fluids cause contamination due to contacting the well wall and then invading into the near-well portion of the reservoir, which leads to the decline of reservoir permeability and affects the production capacity.^{1–4} Working fluid contamination is a relatively common form of reservoir damage; in general, working fluid damage is mainly divided into solid-phase damage and liquid-phase damage.⁵ At present, some progress has been made in indoor simulations of reservoir drilling fluid damage. For example, Feng et al.⁶ used the permeability model established by the transient pressure conduction method to solve the solution of the model by combining it with the Raschel transform. The damage law of drilling fluid on the gram-deep dense sandstone matrix was quantitatively analyzed by using a pressure conduction permeability meter, and this research result provides a new idea for evaluating the injury of incoming fluids. In recent years, with the continuous improvement and development of science and technology, many scholars have conducted meticulous research on reservoir damage. Cui et al.⁷ used a drilling mud indoor experiment to study the damage mechanism of drilling mud in a reservoir in Qingshui Basin. It was found that the main types of drilling mud reservoir damage are filtrate and particles, and it was suggested to use nonsolid phase drilling mud.^{8,9} In

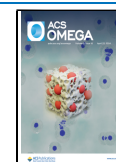
addition, the types of drilling mud reservoir damage are coal dust and particle transportation, and to mitigate their damage, plugging agents can be used to seal the formation and control the chance of contact between the filtrate and the coal bed. In order to evaluate the extent of drilling mud damage to the reservoir, Guo et al.¹⁰ divided the core into matrix core and fracture-type core and chose the CT scanner to study the depth of solid-phase intrusion of mud and the distribution state after intrusion. Fracture type core intrusion characteristics from the three-dimensional image were intercepted from the top view, parallel to the fracture, and perpendicular to the fracture in three different directions scanning the map. The experimental results of the mud contamination of the core can be seen in the obvious solid-phase contamination area, but that mainly concentrated in the injection end of a certain distance from the edge of the core is basically not contaminated; the closer the fracture and the deeper the color, the more serious is

Received: January 11, 2024

Revised: March 22, 2024

Accepted: March 27, 2024

Published: April 10, 2024



the contamination. The crack is the main flow channel, and the pollution is mainly concentrated in the crack. All of the above methods illustrate the drilling mud damage from a single perspective, but they cannot precisely characterize the spatial damage of the working fluid.

At the same time, there are also many scholars from different aspects of reservoir damage conducting a lot of research, Dong et al.¹¹ developed an NDF-1 type well washing fluid;¹² the well washing fluid has low-permeability sandstone gas reservoirs from strong hydrophilic to weak hydrophilic, eliminating the capillary pressure of the reservoir, dissolving some of the incoming solid phases, dismantling the blockage, and thus improving the efficiency of gas drive water. Its indoor experiments show that the well washing fluid NDF-1 can cause field damage after the core permeability recovery rate is significantly improved, and the average recovery rate increase reached 133.45%. Chen et al.¹³ developed a foam steering agent that is easily soluble in an oil and water two-phase medium, has high temperature stability, and is noncorrosive to carbonate rock. With 15% hydrochloric acid and 10% acetic acid in 100 mL/min under the dynamic dissolution experiments and water-based foam penetration into the rock matrix and tectonic surfaces, nitrogen ventilation into the mixing makes the foam occur; with the foam compressive aggregation, more pressure of acid, and acid steering breakthrough of the low-permeability filter cake, the foam is persistent, penetration distance is long, and the steering rate is high. However, the foam thermal stability is poor and sensitive to temperature and has limited influence in engineering applications.^{14,15} Guo et al.¹⁶ studied the nonhomogeneous reservoir of Longwangmiao in Sichuan Basin; they drew on the volumetric fracturing technology, using the reduced-resistant acid as the main acid, under high displacement to reduce friction, and propping open the natural fractures, so that the acid filtration loss along the fractures was deep into the reservoir, relying on its high reactivity to dissolve the foreign pollutants in the fracture and the primary and secondary fill minerals. It can indeed establish a few mesh flow channels with considerable flow-conducting ability to eliminate near-well damage. However, it can only be established based on high purity of reservoir carbonate rock, and there is also the problem of excessive acid consumption.

It can be seen that the research on the damage of the wellbore working fluid to the reservoir has made some progress, but there is no complete evaluation system for the injury characterization part of the working fluid; most of them only illustrate the degree of damage by a single means. In this paper, the spatial damage characteristics of wellbore working fluids on sandstone reservoirs are investigated by combining various indoor experiments and characterization methods, taking the K75 reservoir as an example. A set of multifunctional and low-corrosion composite plugging fluid systems is optimized by dissolution and corrosion experiments on mud cake and reservoir rock powder derived from the filtration loss experiments of the wellbore working fluid used in the K75 reservoir. Finally, the dynamic flow plugging experiment evaluated the dynamic plugging effect of the composite plugging fluid.

2. EXPERIMENTAL SECTION

2.1. Instruments and Materials. **2.1.1. Instruments.** The experimental study of spatial damage characteristics of working fluid was conducted using the dynamic filtration loss apparatus of fracturing an acidized working fluid (Figure 1: Bearing

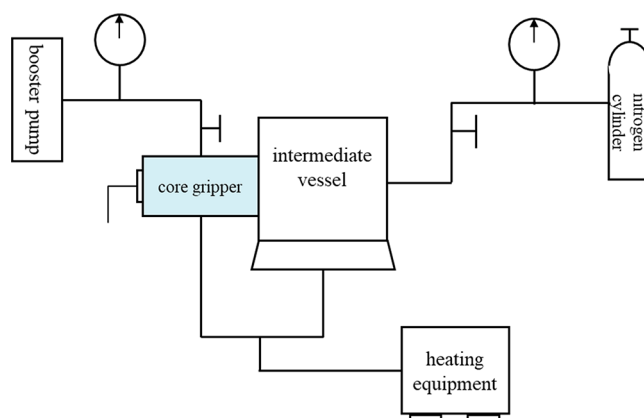


Figure 1. Flowchart of working fluid space damage experiment.

pressure: 20 MPa; Temperature resistance: 150 °C). The dynamic unblocking experiments of the unblocking fluid system were carried out using the core dynamic replacement experimental device (Figure 2: Bearing pressure: 100 MPa;

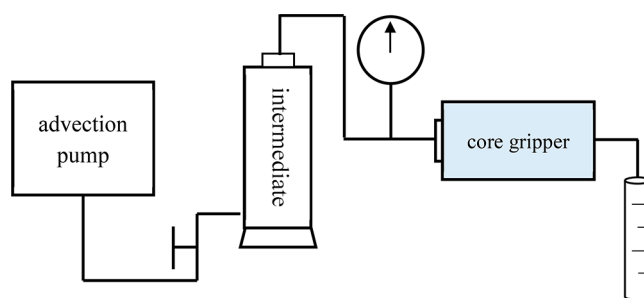


Figure 2. Dynamic unblocking flowchart.

Temperature resistance: 180 °C). The depth and extent of core intrusion were analyzed by using a continuous core scanner (Autoscan, GIocom Inc., USA). The mineral composition of the core was analyzed using an X-ray diffractometer (X'Pert Pro, Panaco Inc., Netherlands, Diffraction angles from 5° to 90°).

2.1.2. Materials. The experimental damage working fluids were drilling fluid (density: 1.4 g/cm³; viscosity: 96 mPa·s), completion fluid (density: 1.9 g/cm³; viscosity: 408 mPa·s), and perforating fluid (density: 1.08 g/cm³; viscosity: 27 mPa·s) provided on site. The four steels P110, 3CrP110, 13CrP110, and L480 were purchased from Shengxin Technology Co. Hydrochloric acid, earth acid, fluoboric acid, polyhydrogen acid, and solid acid were analytically pure and were purchased from Chengdu Cologne Reagent Co. The other additives, including NW-18, ZP-5, HS-3, and TW-7, were manufactured in the laboratory.

The experimental cores were taken from the Ke75 reservoir, which has a low permeability (0.037–0.58mD). The mineral composition of the core was obtained as shown in Table 1. The main mineral components are clay, quartz, and plagioclase.

2.2. Experimental Methods. **2.2.1. Working Fluid Space Damage Experiment.** In order to clarify the damage of the wellbore working fluid to the reservoir, a filtration loss experiment was carried out on the core of the Ke75 reservoir using a high temperature and high pressure filtration loss instrument to simulate the damage of working fluid to the

Table 1. Mineral Composition Analysis of Rock Core

core no.	well no.	content (%)								
		clay	barite	quartz	potash	plagioclase	calcite	dolomite	limonite	pyrite
1#; 2#; 3#	MH123	39.1	0.0	32.0	0.0	22.5	6.5	0.0	0.0	0.0
4#; 5#; 6#	Ke004	33.1	0.0	26.7	5.4	34.8	0.0	0.0	0.0	0.0

Table 2. Degree of Core Damage in Block Ke75

no.	length/cm	pressure/MPa	type	diameter/cm	K_0 /mD	K_1 /mD	R_1 /%
1#	5.033	3.5	Drilling fluid	2.467	0.16	0.106	33.5
2#	5.065	8	Drilling fluid	2.485	0.58	0.207	64.1
3#	5.011	10	Drilling fluid	2.497	0.09	0.023	74.5
4#	5.084	3.5	Drilling fluid + Completion fluid + Perforating fluid	2.502	0.037	0.017	34.9
5#	5.012	8	Drilling fluid + Completion fluid + Perforating fluid	2.515	0.05	0.015	69.7
6#	5.009	10	Drilling fluid + Completion fluid + Perforating fluid	2.513	0.19	0.031	83.6

reservoir in the field. The experiment was carried out at reservoir temperature (76 °C) and different circulating differential pressures (3.5, 8.0, and 10 MPa), and the specific experimental procedures are as follows.

- (1) Preparation stage: Put the core into the core holder after numbering and labeling the direction. Pour the prepared working fluid into the middle container and connect the experimental pipeline.
- (2) Enclosure pressure and temperature loading: When the enclosure pressure reaches the set value, close the enclosure valve. Turn on the heating device, set the experimental temperature, and wait for heating to the experimental temperature.
- (3) Experimental stage: open the gas cylinder to pressurize to the experimental pressure, push the working fluid through the core, and observe the drilling fluid outflow at the outlet side of the core gripper. Timing is done when the drilling fluid starts to flow out, and the cycle time is 120 min.
- (4) Data processing: the degree of damage to the core by the working fluid is calculated in eq 1.

$$R_1 = \frac{K_0 - K_1}{K_0} \times 100\% \quad (1)$$

where R_1 is the degree of damage; K_0 is original permeability of the core, mD; and K_1 is permeability of the core after damage, mD.

2.2.2. Continuous Scanning Test of Cores. A comparison of permeability changes before and after the core can evaluate the overall degree of damage to the core, but the specific range of damage to the core by the working fluid is still unclear; it is necessary to scan the core before and after the damage through the core continuous scanning equipment, and by comparing the changes in the scanning results before and after the damage to the core, the specific range of damage to the core can be reflected. The specific realization method is to use the core continuous scanning system; the core before and after the damage or before and after the unblocking of the core to the same point of the signal can be calculated at the same point of the permeability difference.

2.2.3. Dissolution of Rock Dust and Mud Cake. In order to optimize the adaptable composite plugging liquid system, the main components of the basic composite plugging liquid system were first selected through the mineral composition of the core, and then, the composite plugging liquid system was

further optimized through the dissolution experiment of the mud cake. The specific experimental steps are shown below.

- (1) Preparation stage: the core and mud cake are crushed, sieved, and dried, and the filter paper is dried and weighed. The core and mud cake are added to the plugging solution according to the mass ratio of 1:10.
- (2) Experimental stage: 2 g of scale samples and 20 g of unblocking solution were put in a beaker in a 76 °C water bath, and the reaction was filtered, dried, and weighed after 2 h.
- (3) Data processing: using the weight loss method to determine the dissolution rate of acid on rock powder, according to eq 2.

$$w = \frac{W_0 - W_1}{W_0} \times 100\% \quad (2)$$

where w is the dissolution rate, %; w_0 is the mass of rock flour before dissolution, g; and w_1 is the mass of rock flour after dissolution, g.

2.2.4. Dynamic Unblocking Experiment. In order to simulate the reservoir dynamic unblocking situation, it is necessary to carry out the dynamic simulation experiment of unblocking fluid; the specific experimental steps are as follows.

- (1) Preparation stage: turn on the constant flow pump, replace the piston of the base liquid storage tank, and exclude the air in the pipeline.
- (2) Experimental stage: in accordance with the prefluid–treatment fluid–postfluid injection order, sequentially inverted tanks injected into the experimental liquid, and liquid injection was at any time to observe the changes in the permeability of the core. When the amount of liquid injection reaches the required PV number and the drive is stabilized, the inverted tank is injected with the reference liquid, and the reference liquid is then used to carry out the drive in order to determine the improvement of the permeability of the formation after acidification. Then, the injection of the reference fluid is reversed until the flow rate is stabilized, and the injection is stopped.
- (3) Data processing: the calculation formula for the permeability recovery rate of the core after unblocking compared to the original core is shown in eq 3. The calculation formula of injury contact rate of core after unblocking compared to core after injury is in eq 4.

$$R_2 = \frac{K_2 - K_0}{K_0} \times 100\% \quad (3)$$

$$R_3 = \frac{K_2 - K_1}{K_1} \times 100\% \quad (4)$$

where R_2 is permeability recovery rate, %; R_3 is damage unblocking rate, %; K_0 is original permeability of core, mD; K_1 is permeability of core after damage, mD; K_2 is permeability of core after unblocking, mD.

3. RESULTS AND DISCUSSION

3.1. Study of Spatial Damage Characterization. In accordance with the evaluation method of the working fluid space damage experiment, loss of filtration damage was carried out on the core of the Ke75 reservoir. The cores were injured at 3.0, 5.0, and 10 MPa driving pressure difference, and the degree of core damage was evaluated by the change of gasometric permeability before and after damage; the experimental results are shown in Table 2.

The results shown in Table 2 are the changes in gasometric permeability before and after core damage and the degree of damage to the core by single drilling fluid and sequential working fluid at different pressure differentials. From the results of the degree of damage, when the circulating pressure difference increases, the degree of damage to the core of the single drilling fluid and sequential working fluids (drilling fluid, completion fluid, and perforating fluid) gradually increases under similar permeability conditions. The reason is that under the premise of the same physical properties and the same experimental fluid there will be more foreign fluids and solid phases under the action of high differential pressure, which leads to the increase of the degree of core damage. The extent of core damage by single drilling fluid ranges from 33.5% to 74.5% and the extent of core damage by sequential working fluid ranges from 34.9% to 83.6%. Different core permeability has different degrees of damage, as can be seen in Table 2; the 5 and 6 cores are almost completely plugged. Comparing the damage of single drilling fluid and sequential working fluid, under the conditions of similar permeability and circulating pressure difference, the degree of damage of sequential working fluid is more serious than that of single drilling fluid because the sequential working fluid damages the core for a longer period and there are more foreign fluids and solids invading into the core, which makes the core more seriously clogged. Combining the above experimental data, the contamination of the reservoir by the working fluid is particularly serious during the drilling process, but the extent of core damage cannot be visually characterized only by the change in the permeability before and after the damage.

Further combined with modernized core scanning equipment, continuous scanning of the core before and after the damage and analysis of the point where the permeability of the core did not change during the continuous scanning process can get the damage depth that reaches the core after the working fluid injures the core; Table 3 shows the specific damage depth obtained by the modernized continuous scanning equipment, scanning of the core after replacing a single drilling fluid or a sequence of working fluids at different differential pressures. Figure 3 shows the scanning results of the modernized continuous scanning equipment on the change in permeability of the core before and after damage.

Table 3. Damage Range of Rock Cores under Different Conditions

no.	length/ cm	pressure/ MPa	type	calibre/ cm	depth of damage/ mm
1#	5.033	3.5	Drilling fluids	2.467	12
2#	5.065	8	Drilling fluids	2.485	20
3#	5.011	10	Drilling fluids	2.497	29
4#	5.084	3.5	Drilling fluids + Completion fluids + Perforating fluids	2.502	17
5#	5.012	8	Drilling fluids + Completion fluids + Perforating fluids	2.515	22
6#	5.009	10	Drilling fluids + Completion fluids + Perforating fluids	2.513	34

Comparing the continuous scanning results before and after the core is injured by the working fluid, it can be seen that the permeability of the core decreases after the core is injured by the working fluid, and the permeability of the core at the tail end will no longer change when the internal pores of the core are blocked; by analyzing the points where the permeability of the core does not change, it can be deduced that the depth of the core is injured by the working fluid. Comparison of the core damage range under different differential pressures reveals that, when the circulating differential pressure is increasing, the core damage range also increases, and the damage range of the working fluid to the core is positively correlated with the circulating differential pressure. Comparing the damage range of single drilling fluid and sequential working fluid, the damage range of single drilling fluid is 12–29 mm and the damage range of sequential working fluid is 17–34 mm. The reason the damage range of sequential working fluid is larger than that of single drilling fluid is that, under the condition of increasing circulating differential pressure, the working fluid is easily enters the core and causes damage and is more capable of entering the core. The reason is that, under the condition of increasing circulating pressure difference, the working fluid is more likely to enter the core and cause damage and is more capable of invading the smaller hole throat.

3.2. Optimization and Performance Evaluation of Unblocking Fluid System. In order to get a decongestion fluid system with a good decongestion effect, excellent performance, and suitability for the reservoir, the experiment determines the base acid solution by analyzing the mineral composition of the core and selects a suitable acid solution and its optimal concentration by combining with the experiment of dissolving rock powder and mud cake. Several groups of composite acid solution are obtained by a composite basic acid solution, and the best composite acid solution is selected through the experiment of dissolving rock powder and mud cake by a composite acid solution. Combined with the preferred composite acid solution, a complete unblocking acid solution system is obtained, and after comprehensive performance evaluation, the unblocking acid solution is flow unblocked to the postdamage core; the changes in the core before and after the unblocking (change in permeability, change in continuous scanning) are analyzed to judge the effect of unblocking of the core and to evaluate whether the unblocking acid solution system is able to effectively unblock the postdamage reservoir.

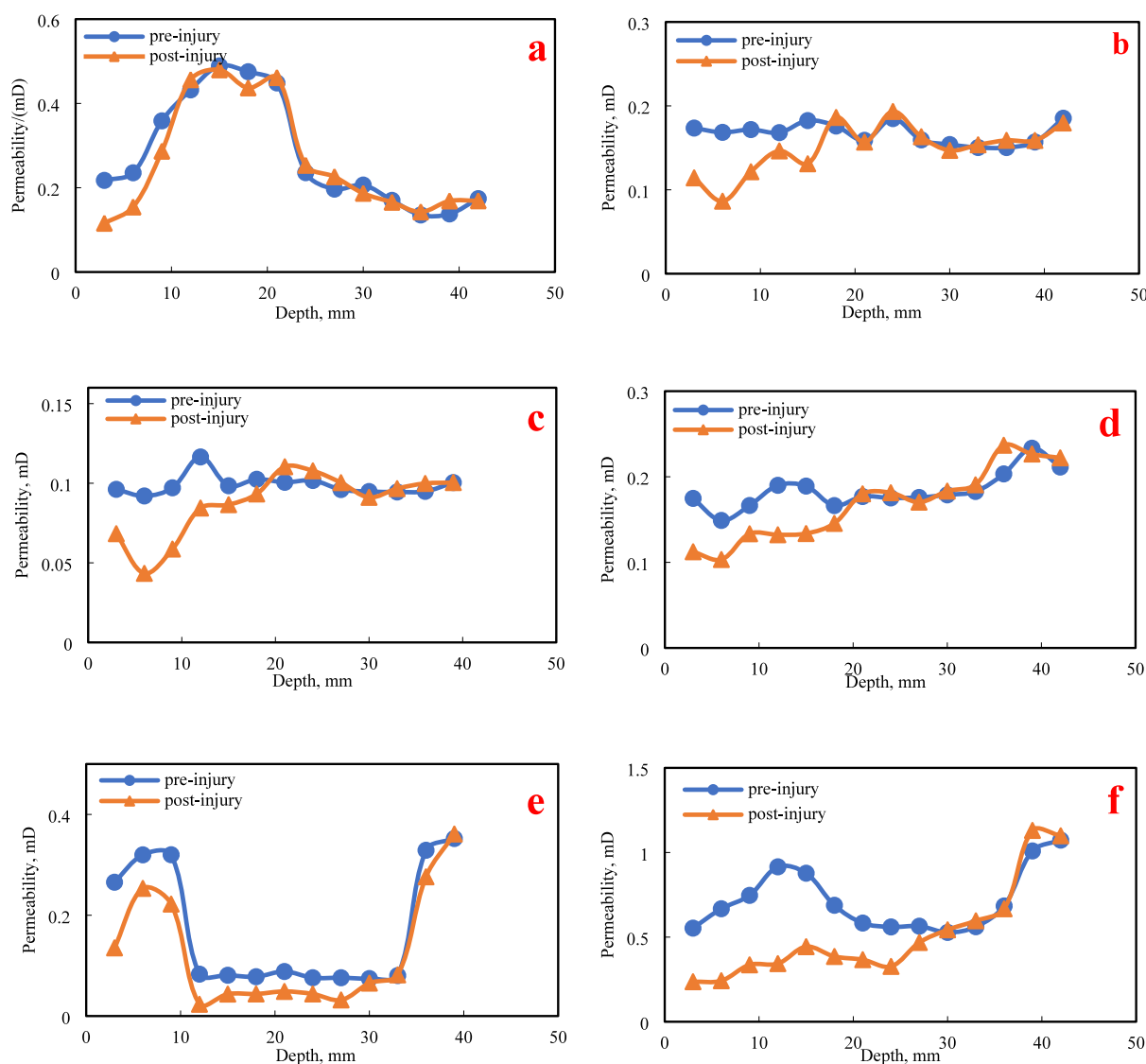


Figure 3. Comparison of consecutive scans of cores 1#–6# before and after damage (a: No. 1#; b: No. 2#; c: No. 3#; d: No. 4#; e: No. 5#; f: No. 6#).

3.2.1. Preferred Type and Concentration of the Main Acid.

According to the mineral composition of the core, five types of acids, namely, hydrochloric acid, earth acid, fluoboric acid, polyhydrogen acid, and solid acid, were initially selected as the basic acid selection. Through the dissolution experiment, the preferred acid and acid concentration, as in Figure 4, show the dissolution rate under different concentrations of various types of basic acid.

Since the working fluid material and core mineral composition contain some carbonate minerals, hydrochloric acid is selected as one of the basic acid choices. As shown in Figure 4a, the core mineral composition contains less calcite, and hydrochloric acid has a low dissolution rate of rock powder, with a dissolution rate of 6.15–10.40%; the dissolution rate increases with the increase of acid concentration, but the increase is not large. It is recommended to choose a hydrochloric acid concentration of 10–15% HCl, which confirms that the carbonate rock content of the formation is not high.

Quartz and feldspar in the mineral composition of the core accounted for 20–35%, which accounted for a relatively high

percentage, and the choice of earth acid as one of the basic acid choices can effectively dissolve some of the silicate minerals in the reservoir pores, properly dissolve the rock skeleton, and increase the porosity near the formation. As shown in Figure 4b, due to the high quartz content in the rock samples, the dissolution rate of earth acid of rock powder in each reservoir is higher, and the dissolution effect is better, with a dissolution rate of 19.75–30.59%. The dissolution rate increases with the acid concentration, but in order to protect the reservoir skeleton, weak acid dissolution is recommended; the selected earth acid concentration is 10% HCl + 0.5–1.5% HF.

In the mineral composition of the core, the content of clay minerals is more than 30%, and HBF_4 acid has a better retardation effect, which can increase the distance of acid action and can stabilize the mudstone to avoid the destruction of stratigraphic structure; so, it is chosen as one of the choices of the basic acidification of HBF_4 acid. As in Figure 4c, under the condition of high clay mineral content, HBF_4 acid has a high dissolution rate to rock powder; the dissolution rate is 8.05–17.79%, and the dissolution rate increases with the

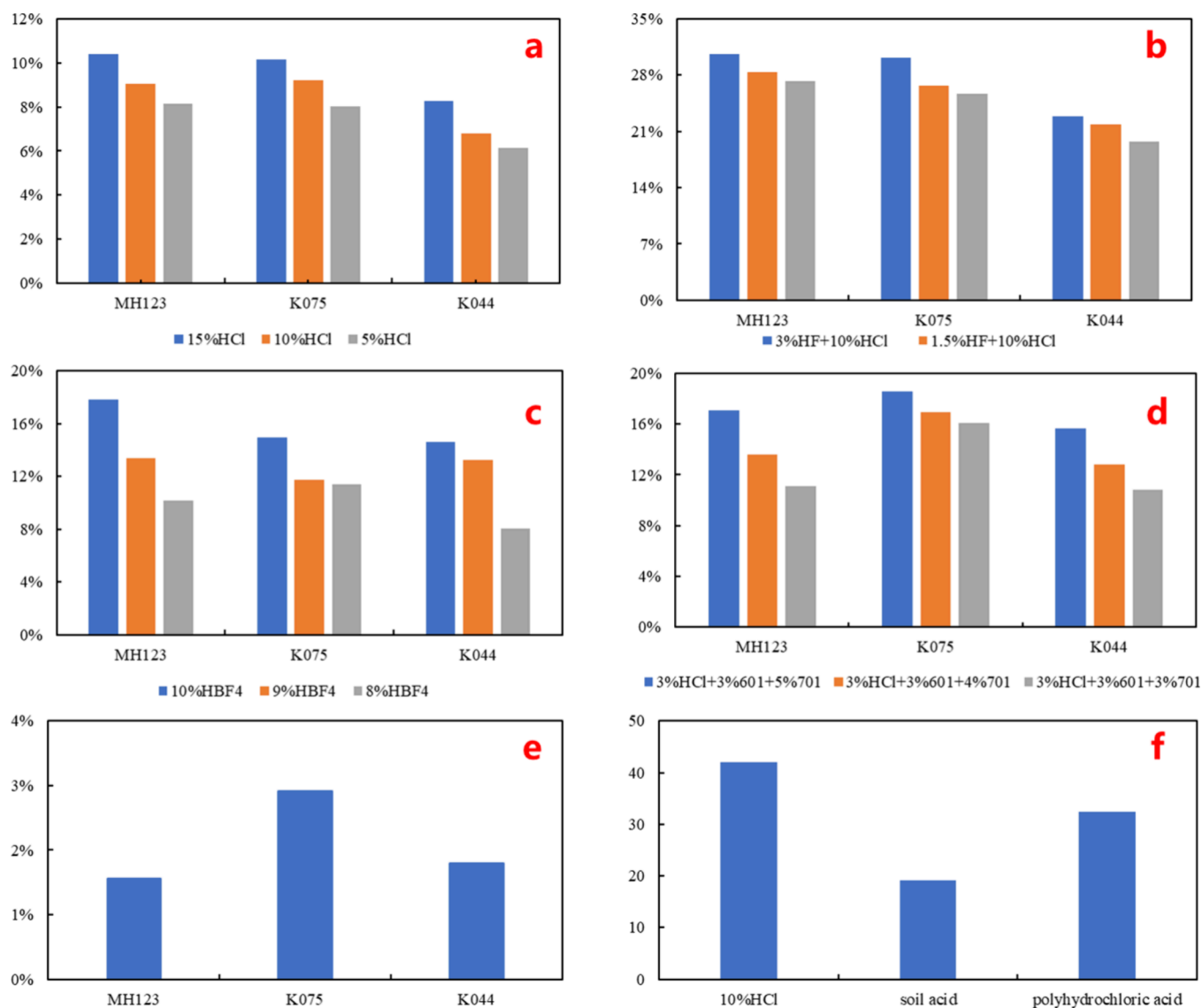


Figure 4. Dissolution effect on rock flour under different types and concentrations of acid solution conditions (a: HCl; b: uric acid; c: HBF₄; d: polyhydrochloric acid; e: solid acid; f: dissolution of mud cake by different acid types).

increase of acid concentration. It is recommended to choose a fluoroboric acid concentration of 8–10%.

Under the action of the stratum environment, the more active primary H⁺ in the polyhydroxyacid first ionizes to generate active H⁺ and provide acidity, followed by secondary ionization, and so on. It ensures the gentle release of H⁺ and the balance of hydrogen ion concentration in the whole process, reduces the damage of strong acidity to the near-well zone, and enhances the ability of the acid solution to unblock the deep part of the well. Meanwhile, it also has strong complexing ability, antiemulsification, and antiacid slag ability itself. Polyhydroxyacid is selected as one of the basic acid fluids; as shown in Figure 4d, polyhydroxyacid has a high dissolution rate of rock powder in each reservoir, with a dissolution rate of 7.1–18.59%, and the dissolution rate of rock powder increases with the increase of the concentration of the acid fluid; the increase is large. It is recommended to select the concentration of polyhydrogen acid as 3% HCl + 3% 601 + 4–5% 701.

In consideration of slow acidization and enhancement of the acidizing distance, solid acid was selected as one of the base

acid choices, as shown in Figure 4e. After 4 h of dissolution, the solid acid has a poor dissolution effect on rock powder, and the dissolution rate is between 1.55% and 2.92%, which cannot achieve the effective decongestion effect; so, the use of solid acid is not recommended.

Since the incoming fluids, such as drilling fluids, contain solid particles, such as barite, it is also necessary to conduct dissolution experiments on the mud cake after acidized leaching. As shown in Figure 4f, various types of suitable concentrations of base acid fluids preferred by rock powder also have good dissolution effects on mud cake.

Due to the good physical properties of the reservoir, in order to protect the reservoir skeleton, the acid needs to be weakly corrosive, and the preferred main acid needs to have a good corrosion effect on the mud cake while having a weak corrosion effect on the rock powder. Therefore, the choice of building a composite acid system can effectively unblock the reservoir at the same time to prevent the physical properties of the reservoir from being destroyed, according to the single-acid erosion experiments, combined with reservoir conditions, and the formulation of three kinds of composite acid system, as

shown in Table 4. It was subjected to rock dust dissolution experiments, and the experimental results are shown in Figure 5.

Table 4. Construction of Composite Acid System

composite acid type	formulas
1#	10% HCl + 8% HBF ₄ + 0.5% polyhydric acid
2#	10% HCl + 10% HBF ₄ + 0.8% polyhydric acid
3#	10% HCl + 8% HBF ₄ + 1.0% polyhydric acid

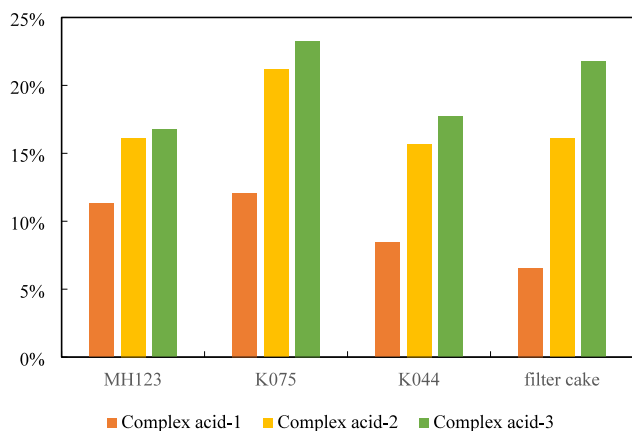


Figure 5. Comparison of dissolving effect of different compound acids on rock powder.

As shown in Figure 5, composite acid-1# has a poor effect on rock powder erosion; the erosion rate is below 12.08%, and at the same time, the erosion effect on mud cake is not satisfactory. The erosion rate is 6.57%. Composite acid-2# and composite acid-3# on the rock powder erosion effect are better at the same time; the mud cake erosion also has a good effect, with erosion rates of 16.1% and 21.8%. However, according to the analysis of the mineral composition of the Ke75 core, the clay mineral content of Ke75 is higher, in order to protect the reservoir skeleton, so we chose the composite acid with a higher fluoroboric acid content and less hydrofluoric acid content as the choice of decongesting acid solution.

3.2.2. Comprehensive Performance Evaluation of Composite Acid Systems. For the composite acid system determined above, the discharge aid and clay stabilizer were added to improve the comprehensive performance of the acid system, and finally, the complete formulation of the composite acid was determined as 10% HCl + 10% HBF₄ + 0.8% polyhydrogen acid + 1% HS-3 + 1% TW-7 + 1% NW-18 + 1% ZP-5. To ensure that the overall comprehensive performance of the composite acid system can meet the standard indicators, the following comprehensive performance evaluation of the composite acid system will be carried out. In order to ensure that the overall comprehensive performance of the composite acid system can meet the requirements of the standard index, the following will be a comprehensive performance evaluation of the composite acid system: including compounding, corrosion inhibition, auxiliary discharge, antiexpansion, iron stabilization, and inhibition of secondary precipitation performance evaluation.

3.2.2.1. Compatibility. The experiment was carried out by leaving the compounded completed acid system at room temperature and 76 °C for 4 h and observing the changes in the acid solution. The results of the experiment are shown in

Figure 6; the acid system is clear and transparent, and there is no delamination, precipitation, and other phenomena. The compatibility is good.



Figure 6. Compatibility of composite acid system.

3.2.2.2. Corrosion Inhibition. In order to ensure that the composite acid system on the metal construction equipment as well as the corrosion of the pipe dwelling is small, there are different types of steel sheets in the composite acid system corrosion experiments. The experimental conditions are static at atmospheric pressure and 76 °C for 4 h. The experimental results are shown in Table 5 and Figure 7.

Table 5. Corrosion of Different Types of Steel Sheets in Composite Acid System

type and dosage of anticorrosive agent	sheet number	corrosion rate/g/(m ² ·h)
1.0% HS-3	3CrP110-245	4.21
	13CrP110-663	2.76
	P110-721	4.61
	L480-252	5.26



Figure 7. Corrosion of steel sheets of different materials by composite acid solution.

As can be seen from Table 5 and Figure 7, the corrosion rate of steel sheets in the composite acid system is low, the corrosion rate of the four types of steel sheets is less than 10 g/(m²·h), and the composite acid system has good corrosion inhibition performance to meet the process requirements. In the field construction, it can alleviate the corrosion caused by the acid on the pipeline and other steel.

3.2.2.3. Performance of Drainage Assistance. The formulated composite acid system was tested for surface tension, and the experimental results are shown in Table 6. According to the composite acid system, the fresh residual acid surface tension measurement found that the surface tension of the composite acid system is lower and its change in the fresh acid and residual acid is not big; the performance is more stable. The auxiliary discharge has a good performance.

3.2.2.4. Antiexpansion Performance. To evaluate the composite acid system antiexpansion performance, antiexpansion agent, distilled water, and kerosene, respectively, were

Table 6. Evaluation of Discharge Aid Performance of Composite Acid Liquid System

type and dosage of auxiliary agents	surface tension (mN/m)			
	fresh acid	average value	residual acid	average value
1.0% ZP-5	24.28	24.31	24.62	24.58
	24.31		24.58	
	24.33	24.54		

added to the expansion of bentonite clay. The experimental results are shown in Table 7; a composite acid system antiexpansion rate of up to 93.23% can effectively inhibit the expansion of clay.

Table 7. Stability Performance Evaluation of Composite Acid Liquid Clay

type of anticomposting agent and dosage	anticomposting rate (%)	average value (%)
1.0% NW-18	94.23	93.23
	93.15	
	92.31	

3.2.2.5. Iron Stability Performance. The iron stabilizing performance of the composite acid system was evaluated to determine if it has better iron stabilizing ability. The experimental results are shown in Table 8, and the amount

Table 8. Evaluation of Iron Ion Stabilizing Ability of Composite Acid Liquid System

type and dosage of iron ion stabilizer	ability to stabilize Fe ³⁺ (mg/mL)	average value (mg/mL)
1.0% TW-7	304	301
	296	
	303	

of iron ions stabilized by the composite acid solution with the addition of iron ion stabilizer is above 240 mg/mL; thus, the composite acid system has a better ability to stabilize iron.

3.2.2.6. Inhibition of Secondary Precipitation. The main types of precipitation that may exist during sandstone acidizing are (1) fluoride precipitation; (2) fluorosilicate precipitation; and (3) hydroxide precipitation. Experiments were conducted to evaluate the precipitation inhibition ability of the composite acid system (three precipitation types are shown in Table 4).

3.2.2.6.1. Fluoride Precipitation. Fluoride precipitates that may be generated during acidizing of sandstone reservoirs mainly include calcium fluoride, magnesium fluoride, etc., which have a small solubility and are white precipitates in the form of frozen gel, which cause damage to the reservoir.

Conventional earth acid acidification will use the front liquid to push some metal ions into the deep part of the formation to reduce the occurrence of precipitation, but the acid solution for acidification is a composite acid; therefore, the composite acid must have a certain chelating ability of metal ions to reduce the occurrence of precipitation. The experimental phenomena of the reaction of different acids with CaCl₂ and the inhibition rate of calcium fluoride precipitation are shown in Table 9 and Figure 8.

**Figure 8.** Reaction of earth and complex acids with CaCl₂ (left: uric acid; right: composite acid).

As can be seen from Table 9 and Figure 8, the conventional earth acid has a low chelating capacity for calcium ions and is highly susceptible to calcium fluoride precipitation, while the composite acid has a high chelating capacity for calcium ions. If the inhibition rate of calcium fluoride precipitation of earth acid is 0, the inhibition rate of calcium fluoride precipitation of composite acid solution is up to more than 70%, which can effectively inhibit calcium fluoride precipitation. The main reason is that the presence of polyhydroxy acid in the composite acid system makes the acid system have a certain chelating effect so that it has the effect of inhibiting Ca²⁺ precipitation.

3.2.2.6.2. Fluorosilicate Precipitation. When the concentration of ions such as Na⁺, K⁺, Ca²⁺, and Mg²⁺ is high enough, fluorosilicates or fluoroaluminum compounds can react with metal ions released from clays and orthoclase feldspars, resulting in the formation of fluorosilicate and fluoroaluminum precipitates, which can cause damage to the reservoir. Therefore, it is necessary to evaluate the inhibition of fluorosilicate precipitation during the experimental process, and the equations of common reactions that generate fluorosilicates and fluoroaluminate are shown below.

From Figure 9 and Table 10, it can be seen that, at room temperature, the earth acid gradually becomes turbid with the increase in the volume of Na₂SiO₃ drops, and a precipitate is generated after adding 4 mL of Na₂SiO₃. The composite acid was clarified after adding a small amount of Na₂SiO₃ and slightly turbid after 5 mL; the inhibition rate of composite acid on fluorosilicate precipitation was more than 60%, so the composite acid solution has better inhibition ability of fluorosilicate precipitation.

Table 9. Reaction Phenomena of Different Acid Solutions with CaCl₂ and Inhibition Rate of Calcium Fluoride Precipitation

acid type	uric acid	composite acid
Addition of CaCl ₂	Solution becomes turbid, precipitation at the bottom of the test tube after standing	No significant change
Adjust pH to 3	Solution becomes more turbid, more precipitation after standing	No significant change
Adjust pH to 5	Solution becomes more turbid, no increase in the amount of precipitation can be observed	Slightly cloudy solution
Heat for 2 h	Precipitation is deposited at the bottom of the test tube, the top of the test tube with pH adjusted, the solution becomes slightly turbid	Slightly cloudy solution
Inhibition %		73



Figure 9. Inhibition of fluorosilicate precipitation in different acid solutions.

Table 10. Reaction Phenomena of Different Acids with Na_2SiO_3 and Inhibition Rate of Fluorosilicate Precipitation

		acid type	
		uric acid	composite acid
Precipitation of mixture after addition of different volumes of sodium silicate solution	1 mL	Clarified and transparent	Clarified and transparent
	2 mL	Clarified and transparent	Clarified and transparent
	3 mL	Slightly muddy	Clarified and transparent
	4 mL	Precipitation	Clarified and transparent
	5 mL	Precipitation	Slightly muddy
	6 mL	Precipitation	Precipitation
Inhibition rate/%			62.5

3.2.2.6.3. Aluminum Fluoride Precipitation. Fluoroaluminate is a precipitate formed after three reactions, the typical reaction equation of which is shown in eqs 5 and 6. Based on the ionic reaction equation to produce fluoroaluminate, it can be concluded that the production of AlF_3 is essential to produce fluoroaluminate precipitation. Therefore, the study of the production of AlF_3 precipitation can indirectly reflect the precipitation of fluoroaluminate. From Figure 10 and Table 11, it can be seen that the inhibition rate of the composite acid on precipitated fluoroaluminate precipitation reached 49.01%, so

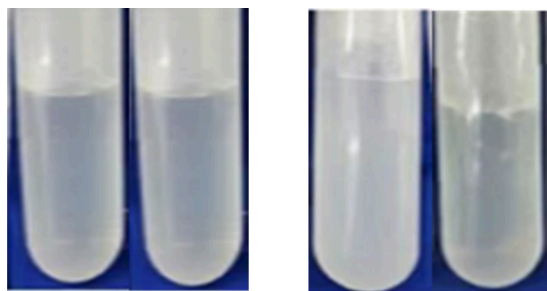


Figure 10. Inhibition of fluoro-aluminate precipitation by different types of acid systems (left: uric acid; right: composite acid).

Table 11. Precipitation Inhibition of Fluoroaluminate under Different Acid Conditions

acid type	inhibition rate (%)
Uric acid	
Composite acid	49.01

it can be reflected that the composite acid system has a strong ability to inhibit the precipitation of fluoroaluminate.



After the above experimental verification, it shows that this set of acid liquid system has good performance in terms of compatibility, corrosion inhibition, auxiliary discharge, anti-expansion, iron stabilization, and inhibition of secondary precipitation. It can meet the industry standard and will not cause a big negative impact on the equipment or itself in the acidizing construction.

3.3. Experimental Study of Dynamic Unblocking. The method of indoor experimental research on the acidification effect is to inject the acidification working fluid into the actual rock core under the simulated conditions of certain temperature and pressure according to a certain construction sequence and analyze the acidification effect according to the change of the permeability of the rock core before and after acidification. A high-temperature and high-pressure acidification effect tester is used to carry out the core rejection experiment. The formula for injecting working fluid in the core replacement experiment is shown in Table 12.

Table 12. Working Fluid Injection Formulas for Core Expulsion Experiments

name of working fluid and injection sequence	decongestion fluid formulation
Base solution: NH_4Cl solution	3% NH_4Cl
Preliminary solution: Hydrochloric acid system	10% HCl + 1% HS-3 + 1% TW-7 + 1% NW-18 + 1% ZP-5
Treatment fluid: Compound acid system	10% HCl + 10% HBF_4 + 0.8% HF + 1% 601 + 11% HS-3 + 1% TW-7 + 1% NW-18 + 1% ZP-5
Postcompletion solution: Hydrochloric acid system	10% HCl + 1% HS-3 + 1% TW-7 + 1% NW-18 + 1% ZP-5

Figures 11 and 12 show the acid flow unblocking diagrams and the corresponding continuous scanning diagrams of predamage permeability, preacidification (postdamage) permeability, and postacidification permeability in the axial direction of the core. From the curves in Figure 11, it can be seen that, as the acid flow unblocking experiment proceeds, the acid liquid reacts continuously with the blockage and the rock skeleton, and when the treatment liquid enters the core, the core permeability recovers faster, indicating that the permeability of the core's blocked pore throats is recovering gradually. Figure 12 illustrates that, in the entire axis of the acid flow through, it can be effective in lifting the working fluid for the damage of the core and, at the same time, can also be partially dissolved in the core, and finally, the core permeability can be restored to the level of the core before the damage above. According to the change of permeability of the core gas

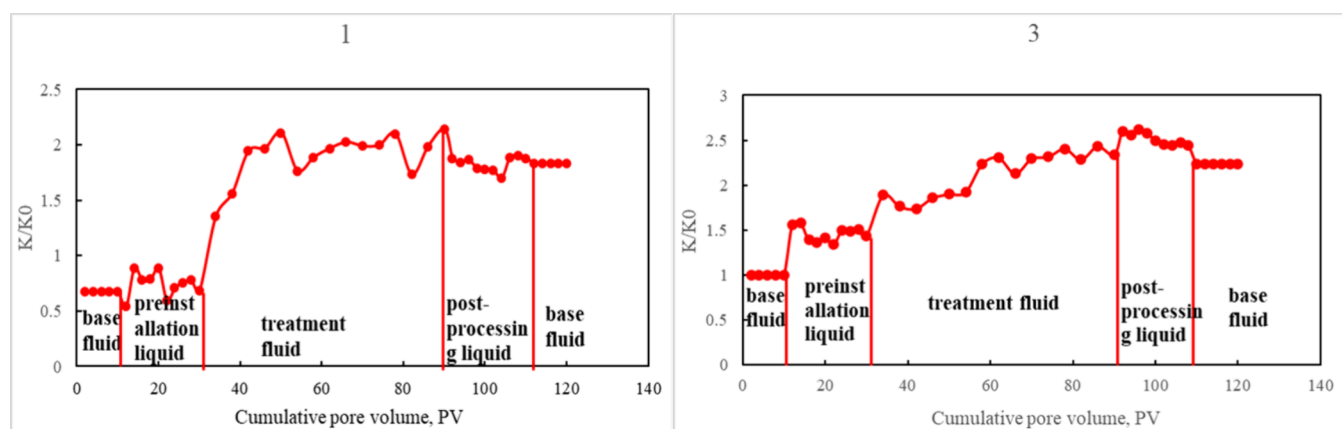


Figure 11. Repellent acid flow curves for cores with different permeabilities.

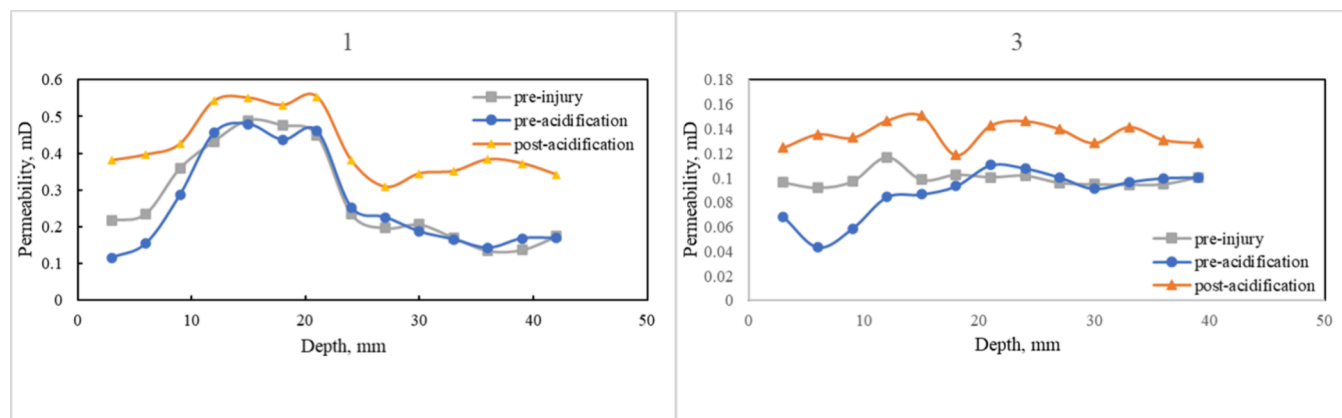


Figure 12. Results of CT continuous scanning experiments before and after damage, unblocking cores with different permeabilities.

Table 13. Changes in Permeability before and after Core Damage Decontamination

no.	replacement pressure/MPa	type	K_0 /mD	K_1 /mD	K_2 /mD	R_2 /%	R_3 /%
1#	3.5	Drilling Fluids	0.16	0.106	0.155	97.04	146.47
4#	3.5	Drilling Fluids + Completion Fluids + Perforating Fluids	0.037	0.0169	0.035	93.95	205.68
2#	8	Drilling Fluids	0.58	0.2072	0.553	95.37	266.96
5#	8	Drilling Fluids + Completion Fluids + Perforating Fluids	0.05	0.0146	0.045	90.26	309.12
3#	10	Drilling Fluids	0.09	0.0231	0.099	109.59	426.99
6#	10	Drilling Fluids + Completion Fluids + Perforating Fluids	0.19	0.031	0.173	91.03	557.95

measurement before and after decongestion, we can roughly understand the degree of core recovery; combined with the results of continuous scanning before and after decongestion, we can more accurately reflect the degree of recovery of the core after decongestion.

Table 13 shows the core gas permeability before and after core damage and before and after decongestion, and the core permeability recovery rate and damage release rate are calculated by eqs 3 and 4. From the data in the table, it can be seen that the recovery rate of core permeability is greater than 90%; at the same time, with the increase of drilling differential pressure, the greater is the degree of core damage, the greater is the rate of core damage relief after unblocking, and the greater is the damage relief rate, greater than 100%. It can be proved that this composite acid system has a good recovery effect for the damage condition of this formation. At the same time, the acidized core maintains the original skeleton strength, which avoids sanding and collapse of the formation after acidization.

It can be seen from the acid flow curve (Figure 11) after unblocking and the comparison of the continuous scanning results (Figure 12) before and after unblocking. Due to the high mud content of the K75 experimental core, the composite acid-2 system with more fluoroboric acid content was chosen as the unblocking agent. The results show that the composite acid-2 system can increase the permeability while reducing the level of etching of the rock skeleton and preventing sand out. The unblocking experiments using the present unblocking solution illustrate that it not only effectively lifts the damage of the working fluid but also has a certain dissolution of the core matrix, which jointly improves the permeability of the core after acidification and meets the acidification requirements. Meanwhile, Figure 13^{17–19} compares the unblocking effect given in this paper and existing literature, and the composite unblocking agent in this paper has an excellent unblocking effect.

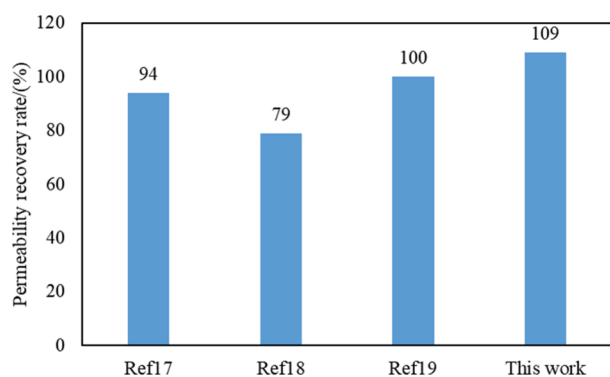


Figure 13. Comparison of dynamic decongestion effect.

4. CONCLUSION

In this study, we investigated the spatial damage characteristic law of wellbore working fluid in a sandstone reservoir and the formulation of a decongestion fluid system after wellbore working fluid injures the reservoir. First, based on the core dynamic loss of the filtration damage experiment, it is clarified that the degree of core damage increases with the increase of differential pressure of the drive. Under the same differential pressure, the damage of sequential working fluid is greater than that of single drilling fluid, in which the damage degree of No. 6# core of Ke75 reservoir reaches about 80%, and the damage depth can reach 43 mm. Then, based on the rock powder dissolution, mud cake dissolution, additive preference, and evaluation, combined with the demand of reservoir characteristics for the acidizing effect, a multifunctional, low corrosion composite acid system for Ke75 block was constructed. The acid formula is 10% HCl + 10% HBF₄ + 0.8% HF + 1% 601 + 1% HS-3 + 1% TW-7 + 1% NW-18 + 1% ZP-5. Meanwhile, the comprehensive performance evaluation of the composite acid liquid system proved that the composite acid liquid system has good compatibility performance, corrosion inhibition performance, ability to stabilize iron ions, and ability to inhibit secondary precipitation. Finally, based on the dynamic unblocking experiment of acid rock flow, the acidizing and unblocking of rock core after damage were carried out. The results show that, under the action of the composite acid liquid system, the damage unblocking rate of Ke75 core reaches 146.47–557.95%, the permeability recovery rate reaches 90.26–109.59%, and the acidizing effect is good.

■ AUTHOR INFORMATION

Corresponding Author

Haoran Fu – School of Petroleum and Natural Gas Engineering, Southwest Petroleum University, Chengdu, Sichuan 610500, China; orcid.org/0009-0003-4644-3819; Email: 13399835448@163.com

Authors

Xiaozhi Xin – Engineering and Technology Research Institute of PetroChina Xinjiang Oilfield Company, Karamay, Xinjiang 834000, China

Jinming Zhao – School of Petroleum and Natural Gas Engineering, Southwest Petroleum University, Chengdu, Sichuan 610500, China

Yiwen Xu – Engineering and Technology Research Institute of PetroChina Xinjiang Oilfield Company, Karamay, Xinjiang 834000, China

Chenghong Jin – Engineering and Technology Research Institute of PetroChina Xinjiang Oilfield Company, Karamay, Xinjiang 834000, China

Zhifeng Luo – School of Petroleum and Natural Gas Engineering, Southwest Petroleum University, Chengdu, Sichuan 610500, China

Yiming Wang – School of Petroleum and Natural Gas Engineering, Southwest Petroleum University, Chengdu, Sichuan 610500, China

Complete contact information is available at:

<https://pubs.acs.org/10.1021/acsomega.4c00252>

Notes

The authors declare no competing financial interest.

■ ACKNOWLEDGMENTS

This work was supported by the Natural Science Foundation of China (No. 51974264).

■ REFERENCES

- (1) Hassan, A.; Murtaza, M.; Alade, O.; Tariq, Z.; Kamal, M. S.; Mahmoud, M. Interactions of drilling and completion fluids during drilling and completion operations. In *Fluid–Solid Interactions in Upstream Oil and Gas Applications*; Developments in Petroleum Science; Elsevier, 2023; Vol. 78, Chapter 3, pp 41–74.
- (2) Katende, A.; Lu, Y.; Bunger, A.; Radonjic, M.; et al. Experimental quantification of the effect of oil based drilling fluid contamination on properties of wellbore cement. *Journal of Natural Gas Science and Engineering* **2020**, *79*, 103328.
- (3) Chai, R.; Liu, Y.; Xue, L.; Rui, Z.; Zhao, R.; Wang, J.; et al. Formation damage of sandstone geothermal reservoirs: During decreased salinity water injection. *Applied Energy* **2022**, *322*, 119465.
- (4) Zhang, Q. Drilling fluids and reservoir protection technology in reservoir section of Wen23 reservoir. *Fault-Block Oil & Gas Field* **2020**, *16* (4), 41–43.
- (5) Fu, M.-t. A Review of Injury Mechanisms and Protection Technologies for Low-Permeability Reservoirs. *Petrochemical Industry Technology* **2019**, *26* (8), 67.
- (6) Feng, Z.-L.; Fujian, Z.; Shicheng, Z.; et al. Evaluation of reservoir matrix fracturing fluid damage based on the pressure pulse method. *Petroleum Geology and Recovery Efficiency* **2018**, *25* (03), 89–94.
- (7) Cui, J.-b.; Chen, B.-w.; Yan, S.-p.; et al. In-use coalbed methane drilling fluids in Qinshui Basin injuring the Qinshui 3# Coalstone: an indoor evaluation. *Oil Drilling & Production Technology* **2013**, *35* (4), 47–50.
- (8) Rasool, M. H.; Zamir, A.; Elraies, K. A.; Ahmad, M.; Ayoub, M.; Abbas, M. A.; et al. A Deep Eutectic Solvent based novel drilling mud with modified rheology for hydrates inhibition in deep water drilling. *J. Pet. Sci. Eng.* **2022**, *211*, 110151.
- (9) Civan, F. Chapter 14 - Drilling-induced near-wellbore formation damage: drilling mud filtrate and solids invasion and mud cake formation. *Reservoir Formation Damage* **2023**, 415–456.
- (10) Zhang, F.-x.; Wang, Z.-h.; Guo, P.; et al. Application of CT technology to study the three-dimensional spatial distribution characteristics of drilling fluid contamination. *Oil Drilling & Production Technology* **2015**, *37* (3), 48–52.
- (11) Dong, H.-w.; Jia, J.; Fan, F.; et al. Research and application of well-washing fluids for relieving drilling fluid injuries in low-permeability sandstone gas formations. **2015**, *32* (4), 40–44.
- (12) Lekomtsev, A.; Kozlov, A.; Kang, W.; Dengaev, A.; et al. Designing of a washing composition model to conduct the hot flushing wells producing paraffin crude oil. *J. Pet. Sci. Eng.* **2022**, *217*, 110923.
- (13) Chen, X.; Zhao, L.; Liu, P.; Du, J.; Wang, Q.; An, Q.; Chang, B.; Luo, Z.; Zhang, N.; et al. Experimental study and field verification

of fracturing technique using a thermo-responsive diverting agent. *Journal of Natural Gas Science and Engineering* **2021**, *92*, 103993.

(14) Su, X.; Qi, N.; Shi, X.; Zhang, Z.; Zhang, Z.; Luo, P.; Yu, Z.; et al. Feasibility of foamed acid treatment in upper stimulation of fractured-vuggy dolomite reservoirs with bottom water. *Geoenergy Science and Engineering* **2023**, *224*, 211552.

(15) Qiao, T.-j.; Zhang, Y.-c.; Cen, L.; et al. Understanding the adaptability of foam acidizing process to low-pressure fractured reservoirs in central Sichuan Province. *Drilling & Production Technology* **2003**, 103–105.

(16) Guo, J.-c.; Cong, L.; Xiao, Y.; et al. Reservoir modification technology for maximizing the reduction of skin factor in Longwangmiao Formation gas reservoirs in the Sichuan Basin. *Natural Gas Industry* **2014**, *34* (3), 97–102.

(17) Yang, X.; Zeng, Y. Optimization of formulation system for acidizing and unblocking in LH oilfield. *Chemical Design Newsletter* **2022**, *48* (3), 43–46.

(18) Yang, Y. Research on multi-round acidizing and unblocking technology for water injection wells. *Petrochemical technology* **2023**, *30* (3), 135–138.

(19) Xu, D.; Ren, K.; Zhao, L.; et al. Research and application of efficient composite acidizing and unblocking technology in offshore thick oil block. *Science Technology and Engineering* **2016**, *16* (27), 157–160.